Merits and limits of the modified Becke-Johnson exchange potential

David Koller, Fabien Tran, and Peter Blaha
Institute of Materials Chemistry, Vienna University of Technology, Getreidemarkt 9/165-TC, A-1060 Vienna, Austria
(Received 15 March 2011; published 31 May 2011)

The modified Becke-Johnson exchange potential [F. Tran and P. Blaha, Phys. Rev. Lett. **102**, 226401 (2009)] (TB-mBJ) is tested on various types of solids which are difficult to describe theoretically: nonmagnetic semiconducting transition-metal oxides and sulfides, metals (Fe, Co, Ni, and Cu), and (anti)ferromagnetic insulators (e.g., $YBa_2Cu_3O_6$). The results for the band gap and other quantities such as the magnetic moment or electric field gradient are analyzed in detail, in particular to have a better understanding of the mechanism which leads to improved (or sometimes worse) results with the TB-mBJ potential compared to the standard local density and generalized gradient approximations.

DOI: 10.1103/PhysRevB.83.195134 PACS number(s): 71.15.Mb, 71.20.−b, 71.27.+a

I. INTRODUCTION

Electronic structure calculations on periodic solids are often performed with the Kohn-Sham[1] (KS) method of density functional theory[2] (DFT) by solving the equations

$$\left(-\frac{1}{2}\nabla^2 + v^{\rm KS}_{{\rm eff},\sigma}(\mathbf{r})\right)\psi_{i,\sigma}(\mathbf{r}) = \epsilon_{i,\sigma}\psi_{i,\sigma}(\mathbf{r}) \qquad (1)$$

for the one-electron wave functions $\psi_{i,\sigma}$. In this equation $v^{\rm KS}_{{\rm eff},\sigma} = v_{\rm ext} + v_{\rm H} + v_{{\rm xc},\sigma}$ is the KS multiplicative effective potential (for spin σ), which is the sum of the external, Hartree, and exchange-correlation (XC) terms. The last term has to be approximated; all other terms can be calculated numerically very accurately. The most popular approximations are the local density approximation (LDA)[1,3] and the PBE[4] version of the generalized gradient approximation (GGA). The XC potential for Eq. (1) is obtained as the functional derivative of the XC-energy functional $E_{\rm xc}$ with respect to the electron density ρ_σ ($v_{{\rm xc},\sigma} = \delta E_{\rm xc}/\delta\rho_\sigma$). This is a fast and reliable theory for ground-state properties which can help to interpret experimental data and has also quite some predictive power. However, one of DFT's main weak sides is the prediction of excited state properties. For instance, the KS band gap of semiconductors and insulators is most of the time severely underestimated. By KS band gap, we mean the difference in energy between the conduction band minimum (CBM) and the valence band maximum (VBM) as obtained from a multiplicative (i.e., common for all orbitals) potential.[5]

In principle, one should not compare the KS band gap with the experimental band gap, which is defined as the ionization potential minus the electron affinity $I - A$. Indeed, even the exact KS band gap differs from the experimental one by the derivative discontinuity $\Delta_{\rm xc}$,[6,7] which can be as large as the KS band gap itself (see, e.g., Refs. 8 and 9). There are indications that the KS band gap calculated with LDA and GGA may not be so different from the exact KS gap,[8] but the problem of these approximations is that $\Delta_{\rm xc}$ is zero. The optimized effective potential (OEP) method applied to the exact exchange functional leads to KS band gaps which are relatively close to the experimental values;[10,11] however this method is computationally expensive and, because of the missing $\Delta_{\rm xc}$, it is maybe in some sense "empirical" to obtain KS band gaps in good agreement with experiment.

There are alternative ways to have an estimate of the experimental band gap. One can use a method which lies outside the KS framework by using a nonmultiplicative potential. Hybrid functionals (e.g., HSE[12]), in which a fraction of exact exchange replaces a fraction of the LDA or GGA exchange, also improve the band gap. However, the hybrid methods are more expensive and also not satisfactory in all cases. Another possibility is the LDA+U[13] method, but it can only be applied to correlated and localized electrons, e.g., $3d$ or $4f$ in transition and rare-earth oxides. Very successful but also very expensive methods are the combination of LDA with dynamical mean-field theory (LDA + DMFT)[14] and of course GW (see Ref. 15 for a recent review). In fact, with such nonmultiplicative potentials (a part of) $\Delta_{\rm xc}$ is contained in the CBM − VBM difference.

Nevertheless, if one wants to stay inside the KS framework and still use a computationally cheap semilocal method that leads to KS band gaps which are close to the experimental band gaps, the potential of Becke and Johnson (BJ)[16] can be a good starting point. The multiplicative BJ potential reads

$$v^{\rm BJ}_{{\rm x},\sigma}(\mathbf{r}) = v^{\rm BR}_{{\rm x},\sigma}(\mathbf{r}) + \frac{1}{\pi}\sqrt{\frac{5}{6}}\sqrt{\frac{t_\sigma(\mathbf{r})}{\rho_\sigma(\mathbf{r})}}, \qquad (2)$$

where $\rho_\sigma = \sum_{i=1}^{N_\sigma}|\psi_{i,\sigma}|^2$ is the electron density, $t_\sigma = (1/2)\sum_{i=1}^{N_\sigma}\nabla\psi^*_{i,\sigma}\cdot\nabla\psi_{i,\sigma}$ is the kinetic-energy density, and

$$v^{\rm BR}_{{\rm x},\sigma}(\mathbf{r}) = -\frac{1}{b_\sigma(\mathbf{r})}\left(1 - e^{-x_\sigma(\mathbf{r})} - \frac{1}{2}x_\sigma(\mathbf{r})e^{-x_\sigma(\mathbf{r})}\right) \qquad (3)$$

is the Becke-Roussel (BR)[17] exchange potential, which was proposed to model the Coulomb potential created by the exchange hole. In Eq. (3), x_σ is determined from a nonlinear equation involving ρ_σ, $\nabla\rho_\sigma$, $\nabla^2\rho_\sigma$, and t_σ, and then b_σ is calculated with $b_\sigma = [x_\sigma^3 e^{-x_\sigma}/(8\pi\rho_\sigma)]^{1/3}$. The asymptotic behavior of $v^{\rm BR}_{{\rm x},\sigma}$ is that of the exact KS exchange potential. The $\sqrt{t/\rho}$ term was introduced to reproduce the step structure of the OEP in atoms and can be considered as a kind of screening term.

The BJ exchange potential has been implemented[18] self-consistently into the WIEN2K code[19] which is based on the full-potential (linearized) augmented plane-wave and local orbitals method to solve the KS equations for periodic systems. In Ref. 18 it was shown that the BJ potential improves over

LDA and PBE for the description of band gaps; i.e., the obtained values for CBM − VBM were larger and hence closer to experiment. However, the improvement was moderate. Further improvement has been achieved by a modified version (TB-mBJ)[20] of the BJ exchange potential which introduces a parameter to change the relative weights of the two terms in the BJ potential:

$$v_{x,\sigma}^{\text{TB-mBJ}}(\mathbf{r}) = c v_{x,\sigma}^{\text{BR}}(\mathbf{r}) + (3c-2)\frac{1}{\pi}\sqrt{\frac{5}{6}}\sqrt{\frac{t_\sigma(\mathbf{r})}{\rho_\sigma(\mathbf{r})}}. \quad (4)$$

The way in which this linear combination is written makes sure that for any value of c the LDA exchange potential is recovered for a constant electron density. For $c = 1$ the original BJ potential is recovered. The actual value of c in the TB-mBJ is calculated for every studied system by

$$c = \alpha + \beta\left(\frac{1}{V_{\text{cell}}}\int_{\text{cell}}\frac{|\nabla\rho(\mathbf{r}')|}{\rho(\mathbf{r}')}d^3r'\right)^{1/2}, \quad (5)$$

where V_{cell} is the unit cell volume and α and β are two free parameters whose values are $\alpha = -0.012$ and $\beta = 1.023$ bohr$^{1/2}$ according to a fit to experimental results. In general, the band gap increases monotonically with respect to c and using Eq. (5) yields satisfying results for many different systems, ranging from small band gap semiconductors to wide gap insulators (even the band gap of 22 eV of Ne can be reproduced fairly well) and transition metal oxides.[20] A drawback of the TB-mBJ potential is that it cannot be obtained as the derivative of a functional as shown in Refs. 21 and 22. Therefore, this potential cannot be used for the calculation of forces which act on the nuclei as required for the optimization of the geometry.

So far, several groups have used the TB-mBJ potential for the calculation of electronic properties of different families of solids and confirmed that TB-mBJ band gaps are improved for a wide range of different materials. Among these works there are the studies of Al-Sawai *et al.*[23] and Feng *et al.*[24] on half-Heusler topological insulators, Feng *et al.*[25] on chalcopyrite semiconductors, Guo and Liu[26] on transition-metal pnictides and chalcogenides, and the numerous calculations reported by Singh *et al.* on halide scintillators,[27] ferroelectric $Bi_4Ti_3O_{12}$,[28] and other solids.[29] Kim *et al.*[30] applied the TB-mBJ potential on III-V semiconductors for the calculation of band gaps and effective masses. While the band gaps improve at least as much as using expensive hybrid DFT methods, the effective masses are not as good, although a considerable improvement compared to PBE calculations has been found.

We also briefly mention published works in which the BJ potential was considered. Kümmel and co-workers[21,31] extended the BJ potential for the calculation of polarizability of molecules. In Refs. 22, 32, and 33, Gaiduk and Staroverov considered more formal aspects of the BJ potential, and in Refs. 34–36, Räsänen and co-workers proposed a correction to the BJ potential.

Finally we mention that the idea to determine an unknown parameter in a XC functional by a density-related property of the specific system under investigation was taken up in Ref. 37, where the fraction of exact exchange in hybrid functionals was not taken as constant, but determined by a very similar expression as Eq. (5). This has led to much better band gaps so that also with hybrid-DFT schemes an accuracy similar to the TB-mBJ potential has been obtained.

However, some questions about the TB-mBJ potential are still open. Where does its strength originate, what are the limitations, is it suitable for metallic systems, or can it also be useful for ground-state properties such as magnetic moments or electron density related properties such as the electric field gradient? In this work we present the results of additional investigations on the merits and weaknesses of the TB-mBJ potential. Since the good performance of TB-mBJ for classical semiconductors is well established, we compare its performance with the benchmark functional PBE on three much more difficult categories of test systems. The three groups are nonmagnetic semiconducting transition-metal oxides and sulfides, where the band gap is of interest; 3d-band metals, where the position of the d bands or the magnetic moment plays an important role; and (anti)ferromagnetic insulators, where both properties are important. For a better understanding of the different results, a detailed analysis of some cases is presented.

II. RESULTS AND DISCUSSION

The calculations were performed with the WIEN2K code.[19] As in our previous work,[20] the TB-mBJ exchange potential was combined with LDA correlation[3] and implemented self-consistently [including Eq. (5)]. For comparison purposes, PBE calculations were also done. The calculations were well converged regarding the integrations in the Brillouin zone and size of the basis set. The two-dimensional plots of the electron densities or potentials were made using XCrySDen.[38]

A. Nonmagnetic transition-metal oxides and sulfides

Table I shows the fundamental band gap of several compounds calculated by PBE and TB-mBJ in comparison with the experimentally measured values and other results from the literature. Generally, there is an improvement for all cases. However, the quality of the improvement is not constant for all cases, but varies a lot. We can find perfect agreement with experiment for HfO_2, but for Cu_2O the band gap is still strongly underestimated. On the other hand, also more sophisticated methods like the hybrid functional HSE, non-self-consistent G_0W_0, or even self-consistent GW are not necessarily better.

Since in a few cases the improvement is relatively modest, we have tried to improve on this. It was mentioned before (see Ref. 20) that the band gap in solids depends nearly linearly on the value of c, and that with increasing c, the band gap increases. Actually, the need to increase "by hand" the value of c to have better agreement with experiment would mean that the present determination of c using Eq. (5) might not be general enough. Using a larger c value [both, the value from Eq. (5) and the optimal value for c are included in Table I], it is possible to reproduce the experimental band gaps in all cases except for Cu_2O. We should mention that Cu_2O seems to be a quite difficult case although formally it is an easy system with a full 3d^{10} shell. Not only is the band gap severely underestimated, but also the electric field

TABLE I. Theoretical and experimental fundamental band gaps [eV]. For comparison, results from the literature which were obtained by other methods (HSE, G_0W_0/GW) are also shown. The value of c obtained from Eq. (5) and the value of c ($c_{\rm opt}$) which leads to the experimental gap are shown in the last two columns. In the G_0W_0/GW column the values from self-consistent GW are indicated with *.

Solid	PBE	TB-mBJ	Expt.	HSE	G_0W_0/GW	c	$c_{\rm opt}$
HfO_2 (monoclinic)	4.09	5.83	5.7[a]		5.45[l]	1.44	1.39
ZnS (zinc blende)	2.10	3.68	3.91[b]	3.49[g]	4.15*[m]	1.28	1.35
ZnO (wurtzite)	0.82	2.71	3.44[b]	2.49[h]	3.8*[m]	1.42	1.64
SiO_2 (quartz)	6.01	8.89	10.30[c]	7.89[c]	9.34[n]	1.47	1.71
$SrTiO_3$ (perovskite)	1.88	2.70	3.25[d]	3.07[i]	5.07[o]	1.41	1.67
TiO_2 (rutile)	1.89	2.57	3.3[e]	3.2[j]	3.34[p]	1.44	1.86
MoS_2 (hexagonal)	0.85	1.07	1.29[c]	1.42[c]		1.22	1.45
ZrO_2 (monoclinic)	3.66	4.73	5.5[a]		4.99[l]	1.42	1.74
Cu_2O (cuprite)	0.53	0.82	2.17[f]	2.12[k]	1.97*[q]	1.32	

[a]Reference 39.
[b]Reference 40.
[c]Reference 37.
[d]Reference 41.
[e]Reference 42.
[f]Reference 43.
[g]Reference 12.
[h]Reference 44.
[i]Reference 45.
[j]Reference 46.
[k]Reference 47.
[l]Reference 48.
[m]Reference 49.
[n]Reference 50.
[o]Reference 51.
[p]Reference 52.
[q]Reference 53.

gradient (EFG) which is a ground state-property and can be directly obtained from the electron density[54] is much too small in PBE calculations (see Fig. 1). With TB-mBJ, when c is increased the band gap increases slightly but never comes close to experiment (Fig. 1) and after a critical value of c, a sudden decrease of the band gap indicates a severe problem for larger c. The calculated EFG of -7.5×10^{21} Vm^{-2} with $c = 1.32$ from Eq. (5) is not too far from experiment, while larger c values lead soon to large errors in the EFG indicating that the TB-mBJ potential with a large c leads to a wrong electron density.

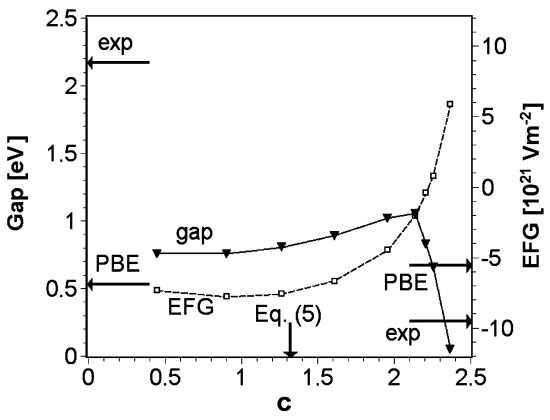

FIG. 1. Variation of the TB-mBJ band gap and Cu EFG in Cu_2O as functions of c. The experimental values for the band gap (Ref. 43) and the EFG (Ref. 54), as well as the band gap and the Cu EFG from PBE, are also shown.

To understand the different performance of TB-mBJ we take a closer look at two examples: $SrTiO_3$ and Cu_2O. Figure 2 shows the electron density of the VBM and the CBM as obtained with the PBE functional. The respective densities obtained with TB-mBJ are very similar and therefore not shown here. Obviously, the VBM density stems from O-2p orbitals, while the CBM originates from Ti-3d states with t_{2g} character and thus also a multiplicative potential can in principle selectively shift these states differently and independently. In fact, when we compare these densities to Fig. 3(a), where the difference between the TB-mBJ and the PBE XC potentials is plotted, we see that in the valence electron region the TB-mBJ potential is more attractive (negative) around both atoms (leading to a stronger localization of the corresponding states), but in addition (and even more importantly) the TB-mBJ potential around Ti is quite aspherical. It is more attractive for Ti-3d-e_g but more repulsive for t_{2g} states and thus shifts the latter upward, leading to a larger band gap. This asphericity comes mainly from the $\sqrt{t/\rho}$ term [Fig. 3(c)], while the BR contribution [Fig. 3(b)] is fairly spherical. Since the $\sqrt{t/\rho}$ term in Eq. (4) is weighted with $3c$, while the BR term is weighted only with c, we can also understand why increasing c increases the band gap.

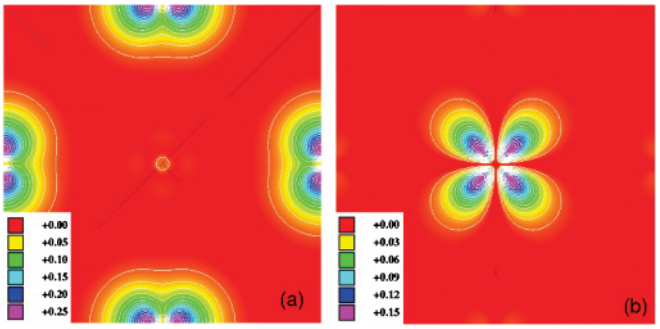

FIG. 2. (Color online) Electron density (in e/bohr^3) of the VBM (a) and the CBM (b) of $SrTiO_3$. The image shows a cross section through the TiO_6 octahedron with Ti in the center and O on the top, bottom, left, and right.

We can now compare this to the situation in Cu_2O. Figure 4 shows the electron density of the VBM and CBM states of Cu_2O in the (011) plane. Both densities are composed mainly of Cu-3d-z^2 orbitals and although there is some difference between the electron density of VBM and CBM, overall they are very similar. Consequently, any orbital-independent potential will not be able to create a large energy difference between these states and thus improve much the band gap with respect to PBE.

B. Metals

By definition, metals do not have a band gap, but still it is interesting to know how the TB-mBJ potential shifts the bands or changes the exchange splitting of some ferromagnetic metals, and whether better agreement with angle-resolved photoemission can be achieved. On the other hand, one must also ask if the Fermi surface or the calculated magnetic moments are still accurate. A first application of TB-mBJ to hcp Gd by Singh[29] was not very promising in this respect.

We start the discussion with fcc Cu, where it is well known that LDA/PBE calculations reproduce very well the Fermi surface but place the Cu-3d bands about 0.5 eV too high in energy (left panel of Fig. 5), while some unoccupied states at the X-point are up to 2 eV too low (right panel of Fig. 5) in comparison to experimental data measured with VLEED.[55] TB-mBJ improves the comparison slightly. The valence band minimum agrees now perfectly with experiment and also the Cu-3d bands are shifted downward, but the shift is too small.

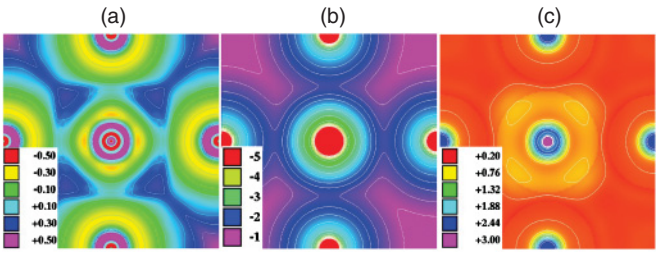

FIG. 3. (Color online) (a) Difference between the TB-mBJ and the PBE XC potentials (in Ry) in $SrTiO_3$. (b) BR term of TB-mBJ potential [Eq. (4)]. (c) $\sqrt{t/\rho}$-term of TB-mBJ potential [Eq. (4)].

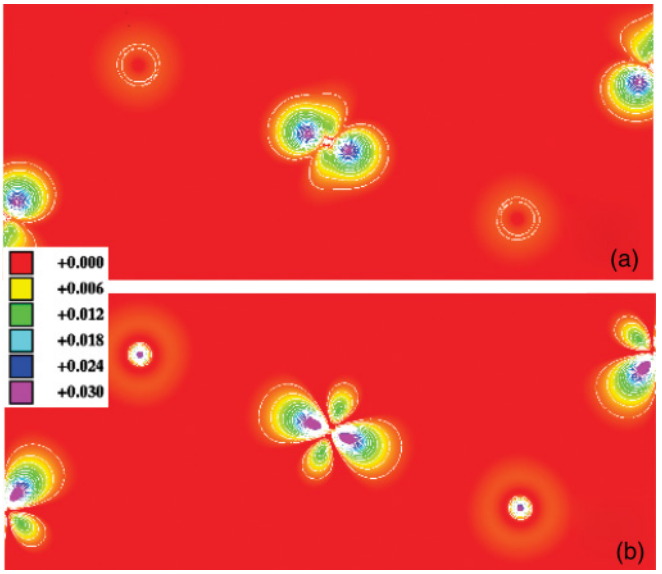

FIG. 4. (Color online) Electron density (in e/bohr^3) of Cu_2O in the (011) plane of the VBM (a) and the CBM (b).

Let us now discuss more demanding cases such as the ferromagnetic metals Fe, Co, and Ni, representing the three classic metallic structures bcc, hcp, and fcc, respectively. It is known (see, e.g., Ref. 56) that the exchange splitting in these metals is not well represented (overestimated) by LDA and GGA, but on the other hand the spin magnetic moments are quite accurately reproduced (Table II). The TB-mBJ potential leads, however, to an increase of the magnetic moments of about 15% and severely overestimates these quantities. In the hcp-Co case, TB-mBJ seems to be a better choice, but Co is known[57] to have a large orbital contribution to the magnetic moment which has to be subtracted from the experimental value (or added to the calculated spin magnetic moment), which means that we face the same problem.

The increased magnetic moments result from a strong increase of the exchange splitting. This makes Fe a strong ferromagnet, where the spin-up d-band is completely filled (as in Ni) (see Fig. 6) and the spin-up Fe-3d-t_{2g} occupation increases while the spin-down 3d occupation decreases.

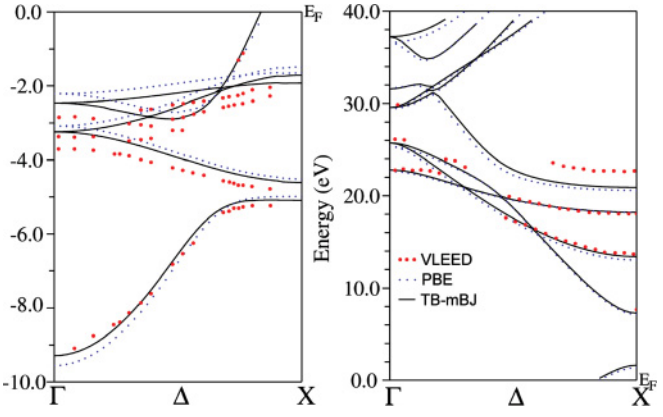

FIG. 5. (Color online) Comparison between PBE and TB-mBJ band structure with VLEED measurements for Cu (Ref. 55).

TABLE II. Comparison between the calculated spin magnetic moments and the experimental total magnetic moments of Fe, Co, and Ni. Values are in μ_B.

Solid	PBE	TB-mBJ	Expt.[a]
Fe (bcc)	2.17	2.49	2.22
Co (hcp)	1.63	1.70	1.72
Ni (fcc)	0.65	0.74	0.606

[a]Reference 40.

The failure to describe ferromagnetic metals by TB-mBJ is not unexpected. The exchange part of TB-mBJ is much stronger than that of LDA/PBE, while the correlation functional (from LDA) has been kept constant and the good error cancellation of LDA/PBE for itinerant metallic systems has been lost. For Fe, it is possible to achieve the correct magnetic moment by adjusting the parameter c in Eq. (4) to a value slightly below 1, while the value calculated from Eq. (5) is $c = 1.19$. However, this leads for instance to a big error in the magnetic hyperfine field (HFF) at the nucleus: $\mathrm{HFF_{PBE}} = 30$ T, $\mathrm{HFF_{TB-mBJ}} = 35$ T, $\mathrm{HFF_{TB\text{-}mBJ},c=0.95} = 12$ T, $\mathrm{HFF_{Expt.}} = 33$ T. TB-mBJ is therefore not recommended in this case.

C. (Anti)Ferromagnetic insulators

Previously, we focused either on the band gap (Sec. II A) or on the magnetic moment (Sec. II B), but here both properties play an important role. The selected examples in this category are antiferromagnetic NiO, CuO, and $YBa_2Cu_3O_6$, as well as ferromagnetic EuO. Table III shows the values for the band gap, the magnetic moment, and the EFG of these materials calculated with PBE and TB-mBJ, together with the experimental values.

Let us start out with NiO, one of the best studied cases where the common semilocal DFT functionals fail. One has to resort to methods like LDA+U[13] where the strong correlations within the 3d shell had to be added "by hand" or highly sophisticated and expensive DMFT calculations.[65] Even standard G_0W_0 calculations improve the gap only slightly, while TB-mBJ leads to very big improvement both for the band gap and the magnetic moment.[20] In Fig. 7 we show the NiO band structure calculated with the PBE and TB-mBJ potentials. In the energy region between -2 and 0 eV there is not much change. These states have a high Ni-3d spin-up and 3d-t_{2g} spin-down character with only modest O-2p contributions. The states where O 2p dominates are located at lower energies. The PBE potential separates them from the Ni-3d bands and places them between -2.2 and -7.5 eV, while in the TB-mBJ calculation they are found between -1.8 and -6.6 eV. The TB-mBJ potential makes the O-2p bands more narrow and shifts them closer to the VBM. The largest difference, however, is in the position of the unoccupied states, which are shifted by about 3 eV (the two flat Ni-3d-e_g spin-down bands) and 2 eV (the parabolic Ni-4s band), respectively. It should be noted that LDA+U (with a suitable value of U) or "hybrid-DFT for correlated electrons only" can also shift the Ni-3d-e_g spin-down bands up, but leave the Ni-4s band

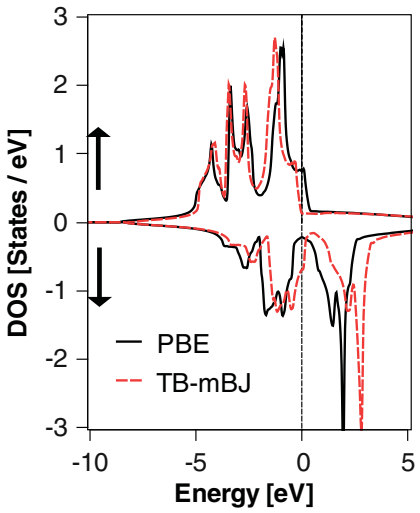

FIG. 6. (Color online) Spin-up and spin-down density of states (in states/spin/cell/eV) of bcc Fe for PBE and TB-mBJ potentials.

TABLE III. Comparison between calculated (PBE and TB-mBJ) and experimental values of the band gap [eV], magnetic moment [μ_B], and electric field gradient [10^{21} V m^{-2}].

	Band Gap			Magnetic Moment			EFG		
Solid	PBE	TB-mBJ	Expt.	PBE	TB-mBJ	Expt.	PBE	TB-mBJ	Expt.
NiO	0.93	4.25	4.0–4.3[a]	1.39	1.76	1.64–1.9[a]			
$YBa_2Cu_3O_6$	0	1.18	1.5[b]	0	0.69	0.66[e]	Cu1: −8.3 Cu2: −3.7	Cu1: −12.8 Cu2: −8.6	Cu1: 11.8[g] Cu2: 9.0[g]
CuO	0.05	2.32	1.4[c]	Cu: 0.38 O: 0.12	Cu: 0.75 O: 0.14	Cu: 0.65[c] O: 0.14[c]	−2.84	−13.97	−7.8[c]
EuO	0	0	0.9[d]	6.99	7.00	6.9[f]			

[a]References given in Ref. 58.
[b]Reference 59.
[c]References given in Ref. 60.
[d]Reference 61.
[e]Reference 62.
[f]Reference 63.
[g]References given in Ref. 64.

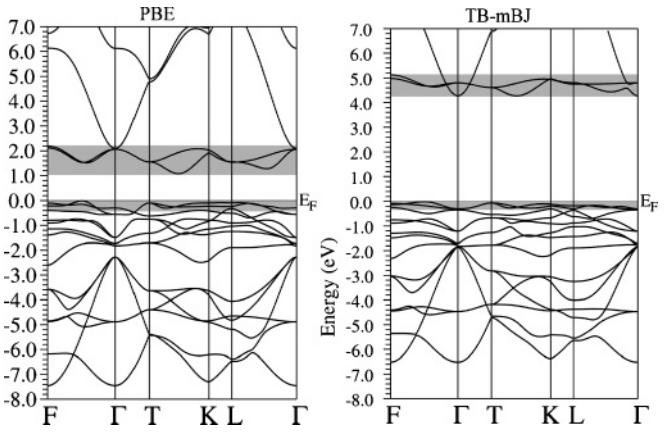

FIG. 7. Comparison of the NiO band structure calculated with PBE and TB-mBJ. The gray regions indicate the states at the valence and conduction bands whose densities are plotted in Fig. 8.

essentially unchanged,[58] while full hybrid-DFT calculations[66] show results similar to those of TB-mBJ.

Figure 8 shows the spin-up density of NiO for states at the VBM and CBM (gray regions in Fig. 7). The VBM of the spin-down Ni atom shows a pronounced $3d$-t_{2g} density with minor contributions from O and the Ni spin-up atom. This density hardly differs between PBE and TB-mBJ calculations. On the other hand, the CBM density has strong Ni-$3d$-e_g spin-down character and the TB-mBJ density shows even less antibonding O-$2p$ and Ni-spin-up character than PBE. This means that both the VBM and CBM states are composed of Ni-$3d$ spin-down states and they differ only in their angular dependency. Thus, the TB-mBJ potential must be able to selectively shift up the $3d$-e_g spin-down states. The difference between the TB-mBJ and PBE spin-up potentials is plotted in Fig. 9. The most important features are not the spherically symmetric oscillations with increasing distance from the nuclei, which are due to more contracted orbitals

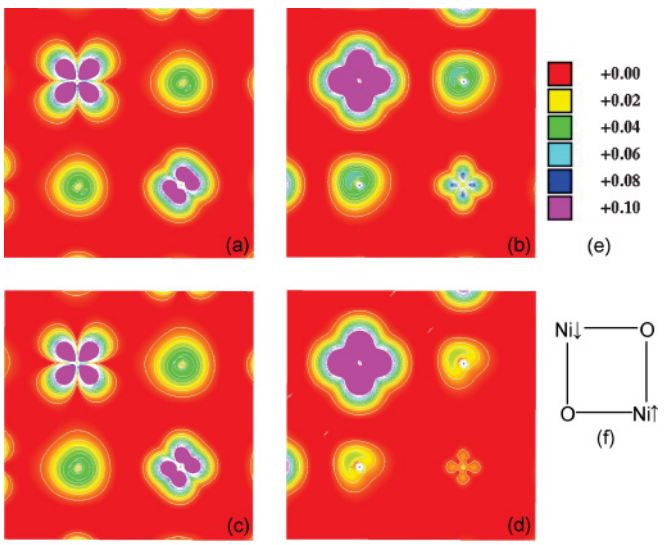

FIG. 8. (Color online) (a) Spin-up electron density in NiO (001) of states in the indicated energy regions in Fig. 7. (a) VBM with PBE. (b) CBM with PBE. (c) VBM with TB-mBJ. (d) CBM with TB-mBJ. (e) Density scale (in e/bohr^3). (f) Position of atoms for (a)–(d).

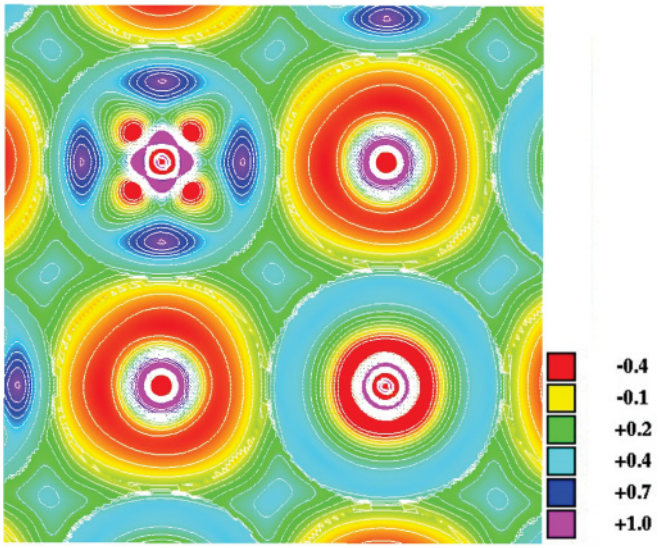

FIG. 9. (Color online) Difference between the TB-mBJ and PBE spin-up XC potentials (in Ry) in the (001) plane of NiO. The positions of atoms are indicated in Fig. 8(f).

in TB-mBJ, but the strong asphericity of the potential around the spin-down Ni atom. This asphericity, which is as large as 1 Ry, causes the larger band gap because it only shifts up the CBM states. In addition, we see a more positive potential in the interstitial region (about 0.2 Ry) which raises the Ni-4s band.

We can analyze which of the two terms of the TB-mBJ exchange potential is responsible for the main effect. The BR and $\sqrt{t/\rho}$ terms are plotted in Fig. 10. While we see also in the BR term some asphericity with a more negative potential in the [110] direction than in [100], the main contribution to the asphericity comes again from the repulsive $\sqrt{t/\rho}$ term, which raises the energy of the $3d$-e_g states. This makes sense since this contribution is proportional to $1/\sqrt{\rho}$ and thus raises the potential in regions with a lower electron density. A similar mechanism is responsible for the increase of the magnetic moments of Fe and Ni and the local magnetic moments of the antiferromagnetic systems. Since only the density of electrons with the same spin is of relevance in the TB-mBJ exchange potential, the spin excess leads to a more attractive potential for electrons with the same spin which in turn leads to an increase of the spin excess and in effect to higher magnetic moments for TB-mBJ. While this is an unwanted effect in the cases of the ferromagnetic metals (Fe, Co, and Ni), here it turns out

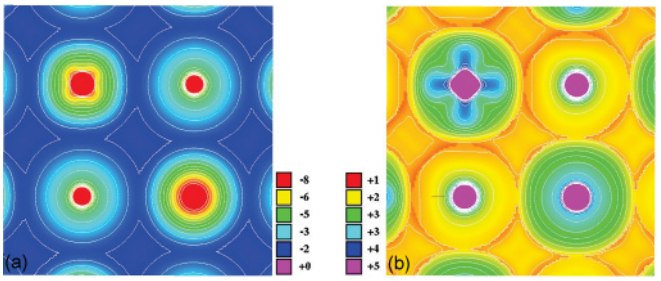

FIG. 10. (Color online) The two contributions to the TB-mBJ exchange potential (in Ry) in NiO in the (001) plane: (a) BR and (b) $\sqrt{t/\rho}$. The positions of atoms are indicated in Fig. 8(f).

TABLE IV. Band gap [eV], magnetic moments [μ_B], and EFG [10^{21} V m^{-2}] of CuO as calculated by PBE and TB-mBJ with $c = 1.41$ [obtained from Eq. (5)] or the value of c [$c_{\rm opt} = 1.22$] which leads to perfect agreement with experiment for the band gap. The references for the experimental values can be found in Ref. 60.

		TB-mBJ		
	PBE	$c = 1.41$	$c_{\rm opt} = 1.22$	Expt.
Band gap	0.05	2.32	1.4	1.4
Cu magnetic moment	0.38	0.75	0.65	0.65
O magnetic moment	0.12	0.14	0.16	0.14
EFG	−2.73	−13.31	−9.94	−7.8

to lead to magnetic moments in much better agreement with experiment than using PBE (see Table III).

The PBE potential fails badly for $YBa_2Cu_3O_6$ (the parent compound of the high-T_c cuprate $YBa_2Cu_3O_{7-x}$), which is an antiferromagnetic insulator. PBE yields a metallic and nonmagnetic ground state (Table III). In contrast, TB-mBJ opens a gap almost as large as in experiment and also gives a correct magnetic moment. In addition the electron density is greatly improved by TB-mBJ as indicated by the EFGs. PBE yields a somewhat too small EFG for the Cu1 site (for definitions see Ref. 67), but in particular the EFG in the CuO_2 plane (Cu2 site) is by more than a factor of two too small. TB-mBJ repopulates slightly the Cu-3d-z^2 at the expense of the 3d-$(x^2 - y^2)$ orbitals and gives EFGs on both Cu sites in perfect agreement with experiment. It should be noted that a similar result can be obtained using LDA+U with a proper choice of U.[67]

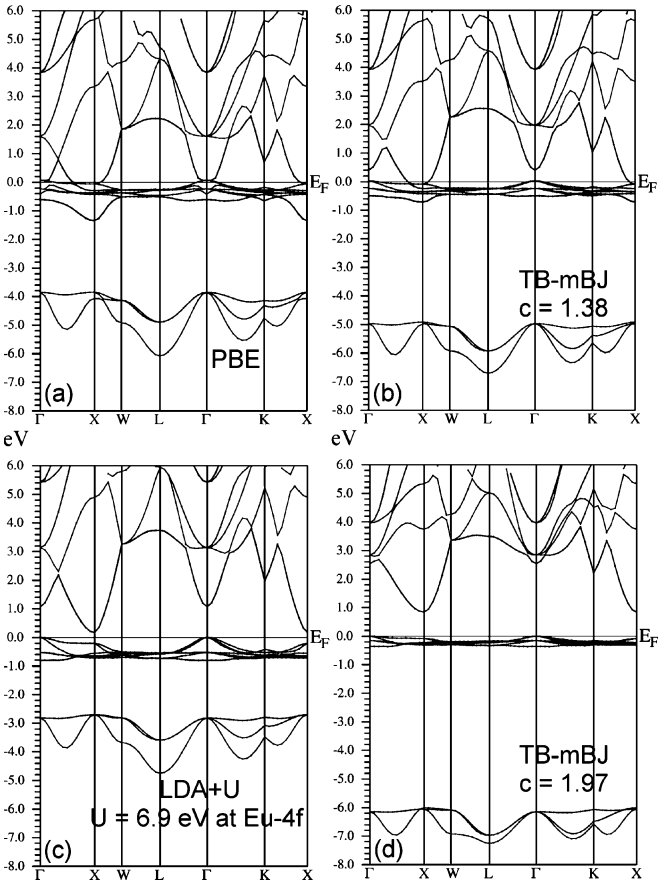

FIG. 11. Band structures of the majority spin in EuO obtained by different methods.

CuO is a system which is at first glance very similar to the cuprates, but here the Cu^{2+} ions have a different O coordination than in the high-T_c materials. An antiferromagnetic ground state and a nonzero band gap are obtained with PBE, but the values of the band gap and of the Cu magnetic moment are by far too small (see Table III). As expected, TB-mBJ increases the magnitude of the values, but now the band gap, the magnetic moment, and the EFG are too large. Apparently, the automatically determined value of $c = 1.41$ [Eq. (5)] is too large. However, by considering the value of c which gives the experimental band gap, $c_{\rm opt} = 1.22$, not only the band gap, but also the magnetic moments and the EFG are very close to experiment (see Table IV). This indicates that it might be useful to search for alternative possibilities to determine self-consistently the value of c in Eq. (4). It should be noted that for CuO also LDA+U (or hybrid-DFT calculations[60]) yields good agreement with experiment only when U (or the mixing factor α) is reduced compared to commonly accepted values for Cu^{2+}.

In the case of EuO both PBE and TB-mBJ give a metallic state (Table III). Figure 11 shows the band structures of the majority spin in EuO calculated with PBE, LDA+U with $U = 6.9$ eV for the Eu-4f orbitals, and TB-mBJ with c obtained from Eq. (5) or the value ($c = c_{\rm opt} = 1.97$) which leads to agreement with experiment for the band gap. The choice of U is based on the linear response approach.[68] All four band structures place the seven spin-up Eu-4f states just below the Fermi level, while the spin-down 4f states are unoccupied. Analyzing the PBE band structure reveals that a band at about 1 eV below the Fermi energy (minimum at −1.3 eV at the X-point) is responsible for the metallic character and this band has predominantly Eu-5d character. The electron density of the states at X near 0 and −1.3 eV are shown in

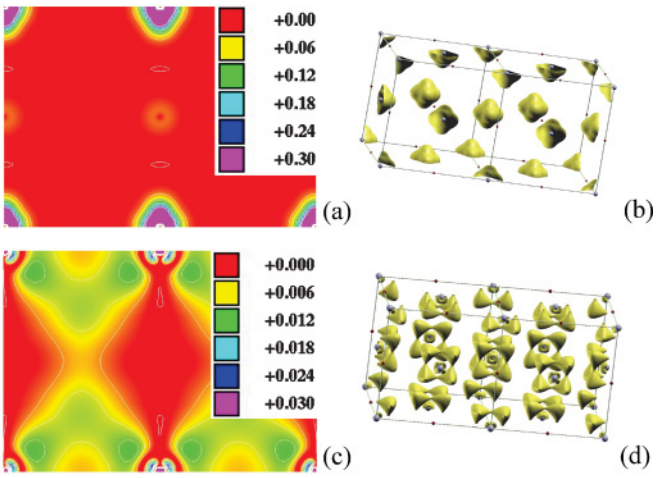

FIG. 12. (Color online) Spin-up electron density according to PBE at the X-point for a state at −0.06 eV: (a) in the (011) plane (Eu atoms on top and bottom and O atoms at the center) and (b) 3D image with 0.03 e/bohr^3 isosurface. Spin-up electron density for a state at −1.3 eV: (c) in the (011) plane and (d) 3D image with 0.0084 e/bohr^3 isosurface.

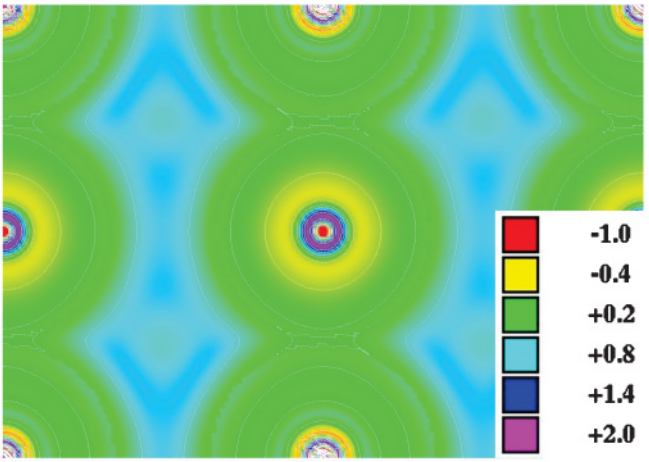

FIG. 13. (Color online) Difference between the TB-mBJ XC potentials (in Ry) obtained with $c = 1.38$ and $c = c_{\text{opt}} = 1.97$ in the (011) plane of EuO.

Fig. 12, where we can see the strongly localized Eu-4f states as well as the delocalized Eu-5d states. Obviously, for an insulating state one has to shift the 5d band up with respect to the 4f states. Standard TB-mBJ [i.e., $c = 1.38$ from Eq. (5)] does this, but the effect is too weak and we still have an overlap at the X point. In addition, TB-mBJ shifts the O-2p states down by about 1 eV and narrows them significantly. LDA+U with a fairly large U opens up a band gap, but it is by far too small compared with experiment because the O-2p bands come too close to the Eu-4f states. One would need an additional U for the O-2p states to solve the problem. The hybrid-DFT methods yield a band gap in EuO which is in good agreement with experiment.[69] As discussed above and shown in Fig. 12, Eu-4f and -5d states have a very different electron density and thus TB-mBJ should be effective, but obviously the self-consistent value of $c = 1.38$ according to Eq. (5) is too small. Similarly to the case of CuO we can try to optimize c in Eq. (4), but in this case we need a larger value of c ($c_{\text{opt}} = 1.97$) to reproduce the experimental gap [see Fig. 11(d)]. The resulting shifts in the band structure can be rationalized by plotting the difference between the TB-mBJ potentials obtained with $c = 1.38$ and $c_{\text{opt}} = 1.97$ as shown in Fig. 13. We see a negative potential around the O atom, which is responsible for the downward shift of the O-2p bands and a positive potential in the interstitial region, where the Eu-5d states have their highest electron density. Again, it is the larger positive $\sqrt{t/\rho}$ term from Eq. (4) that is responsible for the effect.

Overall, the performance of the TB-mBJ potential is excellent for NiO and $YBa_2Cu_3O_6$, but less good for CuO and EuO, where smaller or larger values for c are required to obtain agreement with experiment. It should be mentioned that in a very similar way "nonstandard" values of U in a LDA+U approach are required.

III. CONCLUSIONS AND SUMMARY

The merits and limits of the TB-mBJ potential have been investigated using three groups of test cases: nonmagnetic transition-metal oxides and sulfides, (ferromagnetic) metals, and (anti)ferromagnetic insulators. The results in this study confirm previous reports[20,23,24,26–29] and show that the semilocal TB-mBJ potential is able to yield highly accurate energy band gaps in most semiconductors and insulators. It works not only for the classical sp-type semiconductors, but also for strongly correlated transition-metal compounds such as NiO. The high accuracy and predictive power could be achieved by determining a parameter c uniquely from the electron density of the specific system [Eq. (5)]. Not only the band structure, but also other properties such as the magnetic moment or the electron density, can be accurately described by the TB-mBJ potential. The method is computationally cheap and its quantitative predictive power is often of similar quality (or sometimes better) as much more sophisticated and expensive methods (see also Ref. 37).

It has also been demonstrated why a semilocal, multiplicative potential such as TB-mBJ can increase the band gap and the use of a nonlocal potential is not a necessary condition. It comes from the fact that the electron density (and the corresponding wave functions) of the VBM and CBM are significantly different in their spatial orientation and thus even a multiplicative potential can act differently on these states. The most important ingredient in this respect is the screening $\sqrt{t/\rho}$ term in Eq. (4), whose contribution is adjusted automatically by $|\nabla\rho|/\rho$ by the use of Eq. (5). The $\sqrt{t/\rho}$ term leads to a more positive potential in regions with low density and thus in general it increases the energy of unoccupied states.

However, we have also found and analyzed a few examples for which this approach is not as accurate as desired. In almost all cases one can fix the problem if one uses a different value for c, but then one loses the predictive power. For most of the problematic cases (EuO, but maybe also ZnO, TiO_2, or ZrO_2) a value of c larger than the one calculated from Eq. (5) would be desirable, but for CuO a smaller one yields better agreement with experiment. This leaves some space for improvement in the determination of c. It could be done via a different density-related quantity, such as the reduced density gradient ($|\nabla\rho|/\rho^{4/3}$), or by involving the kinetic energy density t, or by going to a more local determination of c instead of an integral over the unit cell.

We have demonstrated that the use of TB-mBJ for metallic systems seems possible but might be problematic, and in particular for the ferromagnetic metals Fe, Co, and Ni, it leads to, e.g., too large magnetic moments. Most likely, this is due to an insufficient screening of the enhanced exchange (Becke-Roussel) term by a correspondingly better correlation contribution.

The only real problematic case found so far is Cu_2O, where the electron densities of the VBM and CBM extend in very similar spatial regions, which means that a multiplicative potential might never be able to solve this problem, while only self-consistent GW[53] and hybrid functionals,[70] which lead to orbital-dependent potentials, can solve this problem.

ACKNOWLEDGMENTS

This work was supported by Project No. P20271-N17 and the SFB-F41 (ViCoM) of the Austrian Science Fund.

[1] W. Kohn and L. J. Sham, Phys. Rev. **140**, A1133 (1965).
[2] P. Hohenberg and W. Kohn, Phys. Rev. **136**, B864 (1964).
[3] J. P. Perdew and Y. Wang, Phys. Rev. B **45**, 13244 (1992).
[4] J. P. Perdew, K. Burke, and M. Ernzerhof, Phys. Rev. Lett. **77**, 3865 (1996); **78**, 1396 (1997).
[5] S. Kümmel and L. Kronik, Rev. Mod. Phys. **80**, 3 (2008).
[6] J. P. Perdew, R. G. Parr, M. Levy, and J. L. Balduz Jr., Phys. Rev. Lett. **49**, 1691 (1982).
[7] L. J. Sham and M. Schlüter, Phys. Rev. Lett. **51**, 1888 (1983).
[8] M. Grüning, A. Marini, and A. Rubio, J. Chem. Phys. **124**, 154108 (2006).
[9] M. Grüning, A. Marini, and A. Rubio, Phys. Rev. B **74**, 161103(R) (2006).
[10] M. Städele, M. Moukara, J. A. Majewski, P. Vogl, and A. Görling, Phys. Rev. B **59**, 10031 (1999).
[11] E. Engel, Phys. Rev. B **80**, 161205(R) (2009).
[12] J. Heyd, J. E. Peralta, G. E. Scuseria, and R. L. Martin, J. Chem. Phys. **123**, 174101 (2005).
[13] V. I. Anisimov, J. Zaanen, and O. K. Andersen, Phys. Rev. B **44**, 943 (1991).
[14] A. Georges, G. Kotliar, W. Krauth, and M. J. Rozenberg, Rev. Mod. Phys. **68**, 13 (1996).
[15] F. Bechstedt, F. Fuchs, and G. Kresse, Phys. Status Solidi B **246**, 1877 (2009).
[16] A. D. Becke and E. R. Johnson, J. Chem. Phys. **124**, 221101 (2006).
[17] A. D. Becke and M. R. Roussel, Phys. Rev. A **39**, 3761 (1989).
[18] F. Tran, P. Blaha, and K. Schwarz, J. Phys. Condens. Matter **19**, 196208 (2007).
[19] P. Blaha, K. Schwarz, G. K. H. Madsen, D. Kvasnicka, and J. Luitz, WIEN2K: *An Augmented Plane Wave plus Local Orbitals Program for Calculating Crystal Properties* (Vienna University of Technology, Austria, 2001).
[20] F. Tran and P. Blaha, Phys. Rev. Lett. **102**, 226401 (2009).
[21] A. Karolewski, R. Armiento, and S. Kümmel, J. Chem. Theory Comput. **5**, 712 (2009).
[22] A. P. Gaiduk and V. N. Staroverov, J. Chem. Phys. **131**, 044107 (2009).
[23] W. Al-Sawai, H. Lin, R. S. Markiewicz, L. A. Wray, Y. Xia, S.-Y. Xu, M. Z. Hasan, and A. Bansil, Phys. Rev. B **82**, 125208 (2010).
[24] W. Feng, D. Xiao, Y. Zhang, and Y. Yao, Phys. Rev. B **82**, 235121 (2010).
[25] W. Feng, D. Xiao, J. Ding, and Y. Yao, Phys. Rev. Lett. **106**, 016402 (2011).
[26] S.-D. Guo and B.-G. Liu, Europhys. Lett. **93**, 47006 (2011).
[27] D. J. Singh, Phys. Rev. B **82**, 155145 (2010).
[28] D. J. Singh, S. S. A. Seo, and H. N. Lee, Phys. Rev. B **82**, 180103(R) (2010).
[29] D. J. Singh, Phys. Rev. B **82**, 205102 (2010).
[30] Y.-S. Kim, M. Marsman, G. Kresse, F. Tran, and P. Blaha, Phys. Rev. B **82**, 205212 (2010).
[31] R. Armiento, S. Kümmel, and T. Körzdörfer, Phys. Rev. B **77**, 165106 (2008).
[32] A. P. Gaiduk and V. N. Staroverov, J. Chem. Phys. **128**, 204101 (2008).
[33] V. N. Staroverov, J. Chem. Phys. **129**, 134103 (2008).
[34] E. Räsänen, S. Pittalis, and C. R. Proetto, J. Chem. Phys. **132**, 044112 (2010).
[35] S. Pittalis, E. Räsänen, and C. R. Proetto, Phys. Rev. B **81**, 115108 (2010).
[36] M. J. T. Oliveira, E. Räsänen, S. Pittalis, and M. A. L. Marques, J. Chem. Theory Comput. **6**, 3664 (2010).
[37] M. A. L. Marques, J. Vidal, M. J. T. Oliveira, L. Reining, and S. Botti, Phys. Rev. B **83**, 035119 (2011).
[38] A. Kokalj, Comput. Mater. Sci. **28**, 155 (2003).
[39] E. Bersch, S. Rangan, R. A. Bartynski, E. Garfunkel, and E. Vescovo, Phys. Rev. B **78**, 085114 (2008).
[40] C. Kittel, *Introduction to Solid State Physics* (John Wiley & Sons, Inc., New York, 1996), 7th ed.
[41] K. van Benthem, C. Elsässer, and R. H. French, J. Appl. Phys **90**, 6156 (2001).
[42] Y. Tezuka, S. Shin, T. Ishii, T. Ejima, S. Suzuki, and S. Sato, J. Phys. Soc. Jpn. **63**, 347 (1994).
[43] P. W. Baumeister, Phys. Rev. **121**, 359 (1961).
[44] F. Oba, A. Togo, I. Tanaka, J. Paier, and G. Kresse, Phys. Rev. B **77**, 245202 (2008).
[45] R. Wahl, D. Vogtenhuber, and G. Kresse, Phys. Rev. B **78**, 104116 (2008).
[46] P. Wang, Z. Liu, F. Lin, G. Zhou, J. Wu, W. Duan, B.-L. Gu, and S. B. Zhang, Phys. Rev. B **82**, 193103 (2010).
[47] D. O. Scanlon and G. W. Watson, J. Phys. Chem. Lett. **1**, 2582 (2010).
[48] H. Jiang, R. I. Gomez-Abal, P. Rinke, and M. Scheffler, Phys. Rev. B **81**, 085119 (2010).
[49] M. Shishkin, M. Marsman, and G. Kresse, Phys. Rev. Lett. **99**, 246403 (2007).
[50] L. Martin-Samos, G. Roma, P. Rinke, and Y. Limoge, Phys. Rev. Lett. **104**, 075502 (2010).
[51] G. Cappellini, S. Bouette-Russo, B. Amadon, C. Noguera, and F. Finocchi, J. Phys. Condens. Matter **12**, 3671 (2000).
[52] W. Kang and M. S. Hybertsen, Phys. Rev. B **82**, 085203 (2010).
[53] F. Bruneval, N. Vast, L. Reining, M. Izquierdo, F. Sirotti, and N. Barrett, Phys. Rev. Lett. **97**, 267601 (2006).
[54] R. Laskowski, P. Blaha, and K. Schwarz, Phys. Rev. B **67**, 075102 (2003).
[55] V. N. Strocov, R. Claessen, F. Aryasetiawan, P. Blaha, and P. O. Nilsson, Phys. Rev. B **66**, 195104 (2002).
[56] M. van Schilfgaarde, T. Kotani, and S. Faleev, Phys. Rev. Lett. **96**, 226402 (2006).
[57] O. Eriksson, B. Johansson, R. C. Albers, A. M. Boring, and M. S. S. Brooks, Phys. Rev. B **42**, 2707 (1990).
[58] F. Tran, P. Blaha, K. Schwarz, and P. Novák, Phys. Rev. B **74**, 155108 (2006).
[59] G. Yu, C. H. Lee, D. Mihailovic, A. J. Heeger, C. Fincher, N. Herron, and E. M. McCarron, Phys. Rev. B **48**, 7545 (1993).
[60] X. Rocquefelte, M.-H. Whangbo, A. Villesuzanne, S. Jobic, F. Tran, K. Schwarz, and P. Blaha, J. Phys. Condens. Matter **22**, 045502 (2010).
[61] A. Mauger and C. Godart, Phys. Rep. **141**, 51 (1986).
[62] J. M. Tranquada, A. H. Moudden, A. I. Goldman, P. Zolliker, D. E. Cox, G. Shirane, S. K. Sinha, D. Vaknin, D. C. Johnston, M. S. Alvarez, A. J. Jacobson, J. T. Lewandowski, and J. M. Newsam Phys. Rev. B **38**, 2477 (1988).
[63] B. T. Matthias, R. M. Bozorth, and J. H. Van Vleck, Phys. Rev. Lett. **7**, 160 (1961).

[64]K. Schwarz, C. Ambrosch-Draxl, and P. Blaha, Phys. Rev. B **42**, 2051 (1990).
[65]M. Karolak, G. Ulm, T. Wehling, V. Mazurenko, A. Poteryaev, and A. Lichtenstein, J. Electron Spectrosc. Relat. Phenom. **181**, 11 (2010).
[66]M. Marsman, J. Paier, A. Stroppa, and G. Kresse, J. Phys. Condens. Matter **20**, 064201 (2008).
[67]P. Blaha, K. Schwarz, and P. Novák, Int. J. Quantum Chem. **101**, 550 (2005).
[68]S. Q. Shi, C. Y. Ouyang, Q. Fang, J. Q. Shen, W. H. Tang, and C. R. Li, Europhys. Lett. **83**, 69001 (2008).
[69]M. Betzinger, C. Friedrich, and S. Blügel, Phys. Rev. B **81**, 195117 (2010).
[70]F. Tran and P. Blaha, Phys. Rev. B (in press).